



## Open Archive TOULOUSE Archive Ouverte (OATAO)

OATAO is an open access repository that collects the work of Toulouse researchers and makes it freely available over the web where possible.

This is an author-deposited version published in : <http://oatao.univ-toulouse.fr/>  
Eprints ID : 9988

**To link to this article :** DOI:10.1021/tx200406c  
URL : <http://dx.doi.org/10.1021/tx200406c>

**To cite this version :** Hadjeba-Medjdoub, Kheira and Tozlovanu, Mariana and Pfohl-Leszkowicz, Annie and Frenette, Christine and Paugh, Robert J. and Manderville, Richard A. *Structure-activity relationships imply different mechanisms of action for ochratoxin a-mediated cytotoxicity and genotoxicity*. (2012) Chemical Research in Toxicology, vol. 25 (n° 1). pp. 181-190. ISSN 0893-228X

Any correspondence concerning this service should be sent to the repository administrator: [staff-oatao@listes-diff.inp-toulouse.fr](mailto:staff-oatao@listes-diff.inp-toulouse.fr)

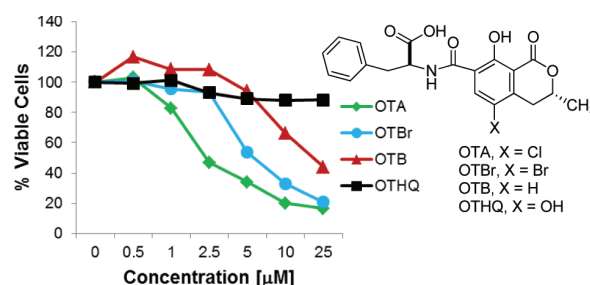
# Structure–Activity Relationships Imply Different Mechanisms of Action for Ochratoxin A-Mediated Cytotoxicity and Genotoxicity

Kheira Hadjeba-Medjdoub,<sup>†,§</sup> Mariana Tozlovanu,<sup>†</sup> Annie Pfohl-Leszkowicz,<sup>\*,†</sup> Christine Frenette,<sup>‡,§</sup> Robert J. Paugh,<sup>‡</sup> and Richard A. Manderville<sup>\*,‡</sup>

<sup>†</sup>Laboratory Chemical Engineering, Department Bioprocess & Microbial System, UMR CNRS/INPT/UPS 5503, ENSA Toulouse, France

<sup>‡</sup>Departments of Chemistry and Toxicology, University of Guelph, Guelph, Ontario, Canada N1G 2W1

**ABSTRACT:** Ochratoxin A (OTA) is a fungal toxin that is classified as a possible human carcinogen based on sufficient evidence for carcinogenicity in animal studies. The toxin is known to promote oxidative DNA damage through production of reactive oxygen species (ROS). The toxin also generates covalent DNA adducts, and it has been difficult to separate the biological effects caused by DNA adduction from that of ROS generation. In the current study, we have derived structure–activity relationships (SAR) for the role of the C5 substituent of OTA (C5–X = Cl) by first comparing the ability of OTA, OTBr (C5–X = Br), OTB (C5–X = H), and OTHQ (C5–X = OH) to photochemically react with GSH and 2'-deoxyguanosine (dG). OTA, OTBr, and OTHQ react covalently with GSH and dG following photoirradiation, while the nonchlorinated OTB does not react photochemically with GSH and dG. These findings correlate with their ability to generate covalent DNA adducts (direct genotoxicity) in human bronchial epithelial cells (WI26) and human kidney (HK2) cells, as evidenced by the <sup>32</sup>P-postlabeling technique. OTB lacks direct genotoxicity, while OTA, OTBr, and OTHQ act as direct genotoxins. In contrast, their cytotoxicity in opossum kidney epithelial cells (OK) and WI26 cells did not show a correlation with photoreactivity. In OK and WI26 cells, OTA, OTBr, and OTB are cytotoxic, while the hydroquinone OTHQ failed to exhibit cytotoxicity. Overall, our data show that the C5–Cl atom of OTA is critical for direct genotoxicity but plays a lesser role in OTA-mediated cytotoxicity. These SARs suggest different mechanisms of action (MOA) for OTA genotoxicity and cytotoxicity and are consistent with recent findings showing OTA mutagenicity to stem from direct genotoxicity, while cytotoxicity is derived from oxidative DNA damage.



## INTRODUCTION

Ochratoxin A (*N*-{[(3*R*)-5-chloro-8-hydroxy-3-methyl-1-oxo-3,4-dihydro-1*H*-isochromen-7-yl]carbonyl}-*L*-phenylalanine, OTA, Figure 1) is a mycotoxin produced by several fungi of *Aspergillus* and *Penicillium* species that is a common contaminant of cereals and agricultural products.<sup>1–5</sup> OTA is nephrotoxic and is a potent renal carcinogen in rats,<sup>6</sup> where it acts as a complete carcinogen (initiator and promoter activity) rather than as a promoter alone.<sup>4,5</sup> OTA is also a potent renal carcinogen in chicks,<sup>7</sup> and the International Agency for Research on Cancer (IARC) has classified OTA as group 2B carcinogen (possible human carcinogen) based on sufficient evidence for carcinogenicity in animal studies.<sup>8</sup>

Given that OTA is a possible human carcinogen present in human foodstuffs, government agencies propose tolerable daily intakes (TDIs) to manage the risk from OTA exposure. Here, the mechanism of action (MOA) by the toxin has a major influence on the methods applied for risk assessment.<sup>9,10</sup> For carcinogens whose MOA involves genotoxicity by covalent DNA adduction (direct mode of genotoxicity), the tumor incidences observed in animals are used to predict potential

tumor incidences in humans exposed to much lower doses. For nongenotoxic chemicals, thresholds based on the induction of cytotoxicity may be defined, and TDIs can be derived using the safety factor methodology.<sup>9,10</sup> The TDI established for OTA by the Joint FAO/WHO Expert Committee on Food Additives uses nephrotoxic effects in pigs and has been set at ~14.28 ng/kg bw/day (100 ng/kg bw/week).<sup>11</sup> Health Canada has recently proposed a more stringent TDI of 4 ng/kg bw/day that considers tumor formation by OTA,<sup>5</sup> given that the characteristics of OTA-induced tumors correspond to those typically observed for genotoxic chemicals.<sup>12,13</sup>

The MOA for OTA has been a controversial issue.<sup>14,15</sup> In mammalian cells, OTA is known to facilitate oxidative DNA damage<sup>16–18</sup> that causes cytotoxicity,<sup>17,19,20</sup> and this MOA has been proposed to play an important role in OTA carcinogenicity.<sup>19,21</sup> This implies that OTA is not a direct genotoxic carcinogen and that a threshold model can be used for OTA risk assessment.<sup>21</sup> However, using the <sup>32</sup>P-postlabeling

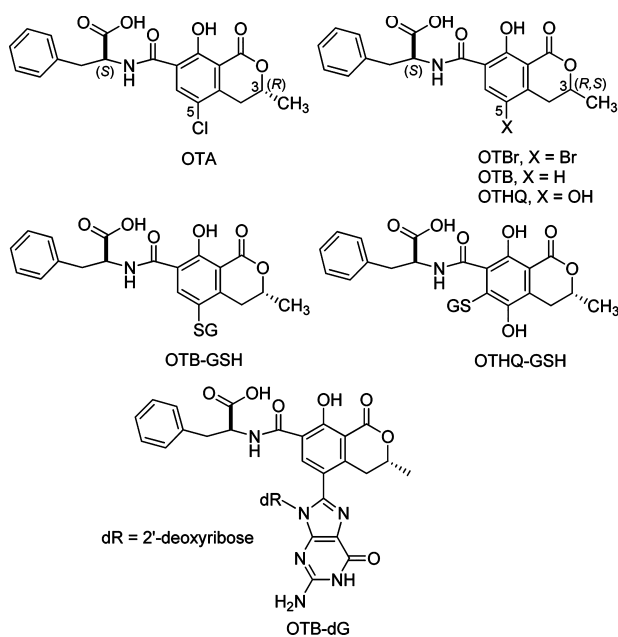


**Figure 1.** Chemical structures of OTA and OTA analogues.

method, OTA has also been shown to facilitate DNA adduct formation,<sup>22–26</sup> and recent LC-MS/MS data support the presence of the *N*-{[(3*R,S*)-8-hydroxy-3-methyl-1-oxo-3,4-dihydro-1*H*-isochromen-7-yl]carbonyl}-*L*-phenylalanine (OTB)-2'-deoxyguanosine (dG) adduct (Figure 1) in rat kidney DNA samples.<sup>27</sup> Hibi and co-workers have also demonstrated the *in vivo* mutagenicity of OTA in male rat kidney.<sup>28</sup> Deletion mutations were observed in the DNA of the target tissue (outer medulla) that were not caused by oxidative DNA damage, suggesting that this indirect MOA does not contribute to induction of deletion mutations nor renal carcinogenesis following OTA exposure of rats.<sup>28</sup> These new findings<sup>27,28</sup> suggest the possible involvement of a direct genotoxic mechanism in OTA-mediated renal carcinogenesis.

To further address the MOA for OTA cytotoxicity and genotoxicity (DNA adduction), we have determined the role of the C5 substituent by comparing the activity of OTA to its analogues shown in Figure 1 (C5–X = Br, OTBr; C5–X = H, OTB; and C5–X = OH, OTHQ). Our data show that the C5-halogen (Br or Cl) is a structural requirement for OTB-dG formation<sup>29</sup> and that its removal to generate OTB abolishes DNA adduct formation in mammalian cells but does not inhibit cytotoxicity. Interestingly, the hydroquinone analogue *N*-{[(3*R,S*)-5,8-dihydroxy-3-methyl-1-oxo-3,4-dihydro-1*H*-isochromen-7-yl]carbonyl}-*L*-phenylalanine (OTHQ) has been found to lack cytotoxicity in mammalian cells, despite being able to react directly with DNA to generate covalent DNA adducts.<sup>30</sup> The structure–activity relationships (SARs) determined in this study imply different MOAs for OTA-mediated cytotoxicity and genotoxicity.

## EXPERIMENTAL PROCEDURES

**Caution:** OTA is toxic and mutagenic and should be handled with proper safety equipment and precautions.

**Materials.** OTA (benzene free, CAS# 303-47-9) was purchased from Sigma (Saint Quentin Fallavier, France). Synthetic samples of bromo-ochratoxin (OTBr),<sup>31</sup> OTB,<sup>31</sup> and OTHQ<sup>32</sup> were available in the laboratory at Guelph, Canada, and were used as mixtures of

diastereomers [3(*R/S*), Figure 1]. Stock solutions of ochratoxins in aqueous 50 mM phosphate buffer, pH 7.4, were prepared as outlined previously.<sup>33,34</sup> Glutathione (GSH) was purchased from Sigma-Aldrich (Oakville, ON), and dG was from ChemGenes (Wilmington, MA). Purchased were the following enzymes: Proteinase K (used as received), RNase A, RNase T1 (boiled for 10 min at 100 °C to destroy DNases), and micrococcal nuclease (dialyzed against deionized water) were from Sigma (Saint Quentin Fallavier, France); spleen phosphodiesterase (centrifuged before use) was from Calbiochem (VWR, France); and nuclease P1 (NP1) and T4 polynucleotide kinase were from Roche diagnostics (Meylan, France). [ $\gamma$ -<sup>32</sup>P-ATP] (444 Tbq/mmol, 6000 Ci/mmol) was from Amersham (Les Ulis, France); Dulbecco's Eagle's minimum essential medium (D-EMEM) and Roswell Park Memorial Institute medium (RPMI) were prepared with Gibco products (Cergy Pontoise, France); phosphate saline buffer, trypsin, fetal calf serum, streptomycin, and penicillin were from Life Technologies (Cergy-Pontoise, France); rotiphenol (phenol saturated with TRIS-HCl, pH 8) was from Rothsichel (Lauterbourg, France); cellulose MN 301 was from Macherey Nagel (Düren, Germany); polyethyleneimine (PEI) was from Corcat (Virginia Chemicals, Portsmouth, VA); Whatman no. 1 paper (ref 6130932) was from VWR (France), and PEI/cellulose TLC plates used for <sup>32</sup>P-postlabeling analyses were prepared in the laboratory at Toulouse, France. All HPLC solvents were of chromatography grade. Water used for buffers, and spectroscopic solutions was obtained from a Milli-Q filtration system (18.2 M $\Omega$ ).

**Methods.** Product isolations were carried out using an Agilent 1200 series HPLC equipped with an autosampler, autocollector, fluorescence, and diode array detector. Separations were performed using an Agilent C-18 5  $\mu$  150 mm  $\times$  4.6 mm column with a flow rate of 0.75 mL/min using the following mobile phase: 70:30 (0.1% formic acid in H<sub>2</sub>O–0.1% formic acid in ACN) to 25:75 in 17 min by a linear gradient. Mass spectra were obtained at the Biological Mass Spectrometry Facility (BMSF) at the University of Guelph using an Agilent 1100 LC-MSD with a single quadrupole detector using electrospray negative ionization (ESI<sup>-</sup>) with a capillary voltage of 3500 V. Data were acquired over the *m/z* range of 50–1000 under normal scan resolution (13 000 *m/z* per s). pH measurements were taken at room temperature with an Accumet 910 pH meter and an Accumet pH Combination Electrode with stirring. UV–visible absorption spectra were recorded on a Cary 300-Bio UV–visible spectrophotometer equipped with a Peltier block-heating unit and temperature controller. Standard 1 cm light path quartz glass cells from Hellma GmbH & Co were used. All UV–vis spectra were recorded with baseline/background correction.

**Photoreactions.** Reaction mixtures (2 mL total volume) of 1 mM ochratoxins (OTA, OTBr, OTB, or OTHQ) in the absence and presence of 15 molar equiv of GSH or 40 molar equiv of dG were prepared in 50 mM phosphate buffer, pH 7.4. The reaction mixtures were irradiated at 350 nm for various lengths of time (2–30 min) using a Rayonet Chamber Reactor, model RPR-200. The 350 nm light source provides an irradiance density of 0.01 M<sub>w</sub>/cm<sup>2</sup>/nm in the 325–375 nm region, which allows selective irradiation of the phenolic ring system of the ochratoxins. Aliquots (100  $\mu$ L) were removed and analyzed by HPLC. For the photodecomposition studies of the ochratoxins, the starting materials (OTA, OTB, OTBr, and OTHQ) were used to construct five-point HPLC calibration curves with UV detection to quantify levels following photoirradiation at 350 nm. For the diastereomers of OTB, OTBr, and OTHQ, the combined peak integrals of the two peaks were utilized. Plotted intensity values have ~5% error determined from three replicate HPLC injections at each irradiation time point (2–30 min). Peaks of interest were also collected, concentrated, and characterized by ESI-MS.

**Cell Culture.** Opossum kidney epithelial cells (OK; ATCC CRL-1840), human bronchial epithelial cells (WI26; ATCC CCL-95.1), and human kidney cells (HK2; CRL-2190) were provided by ATCC (American Type Culture Collection, Manassas, VA). WI26 cells were cultured in RPMI, while OK and HK2 were cultured in D-EMEM medium containing 44 mM NaHCO<sub>3</sub>, 5% fetal bovine serum (FBS), 2% vitamins, 2% nonessential amino acids, 1% streptomycin (100  $\mu$ g/

mL, Gibco), and 1% penicillin (100 U/mL, Gibco) for 48 h at 37 °C under 5% CO<sub>2</sub>. After trypsin digestion, the cells were resuspended in culture medium to obtain 1 × 10<sup>6</sup> cells/mL.

**<sup>32</sup>P-Postlabeling.** WI26 or HK2 cells were treated with 1 μM OTBr or OTB for 1.5, 6, or 24 h. DNA isolation and extraction were carried out as fully described in Tozlovanu et al.<sup>30</sup> The method used for <sup>32</sup>P-postlabeling was that initially described by Reddy and Randerath,<sup>35</sup> with minor modifications outlined in Faucet et al.<sup>26</sup>

**Cytotoxicity.** For cytotoxicity measurements, OK, WI26, or HK2 cells were incubated for 48 h in the presence of 0.5, 1, 2.5, 5, 10, or 25 μM OTA, OTBr, OTB, or OTHQ. Cell viability was assessed using the MTT assay, as described previously.<sup>36</sup> The assay is based on the capacity of living cells to convert the tetrazolium salt into formazan, which absorbs at 570 nm and is positively correlated with cell survival. After one night for the cell adhesion at 37 °C, 10 μL of each ochratoxin was applied for 48 h at 37 °C. At the end of the incubation, 15 μL of MTT (5 mg/mL, Sigma-Aldrich) in phosphate-buffered saline (PBS) was added to the 96-well plates for 4 h at 37 °C. The absorbance at 570 nm was measured with a 96-well plate reader. The results were measured in six independent experiments and were expressed as the percentage of viability (%) with respect to the control (solvent treated cells, 0.1 M HNaCO<sub>3</sub>, pH 7.4, 1% DMSO), according to the following formula: [(absorbance treated cells - absorbance blank)/(absorbance control cells - absorbance blank)] × 100. Statistical analysis was done using the software SPSS 13.

## RESULTS

**Photoreactivity.** We have previously demonstrated that OTA is photoreactive and that the products from the photoreaction provide insight into species that may participate in OTA-mediated DNA damage.<sup>34,37</sup> Figure 2 shows the

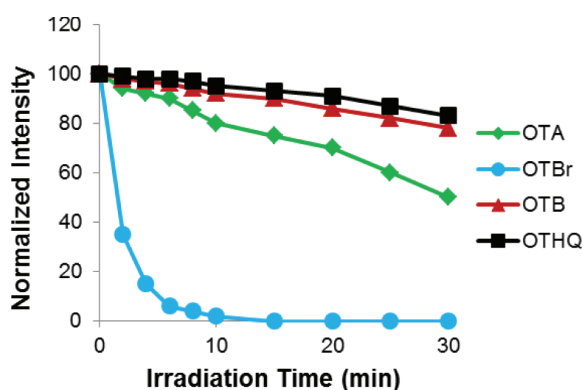


**Figure 2.** HPLC analysis of the photodegradation of ochratoxins (1 mM) in 50 mM phosphate buffer, pH 7.4, over a span of 30 min of irradiation at 350 nm. Plotted values have ~5% error determined from three replicate HPLC injections at each time point.

relative rates of photodecomposition of the ochratoxins (OTA, OTBr, OTB, and OTHQ, Figure 1) following irradiation at 350 nm. OTA decomposes relatively slowly upon UV irradiation in aqueous solutions,<sup>34</sup> and following 30 min of irradiation time, ~50% of the toxin was still present, as evidenced by HPLC analysis. In contrast, the bromo-analogue OTBr had completely photodecomposed following ~10 min of irradiation time, while OTB and OTHQ (~80% still present after 30 min) were more resistant than OTA to photodecomposition.

Further insight into photoreactivity differences for the ochratoxins was obtained by carrying out the photoreactions in the presence of excess GSH. Figure 3 shows HPLC chromatograms for the ochratoxins (1 mM) following photoirradiation (15 min) at 350 nm in the presence of 15 equiv of

GSH. For OTA (Figure 3A), the new product peaks mainly stem from substitution of the C5-Cl atom with an H atom (OTB), OH (OTHQ), or GSH (OTB-GSH). The exception is OTHQ-GSH (Figure 1) that forms by nucleophilic attachment of GSH to the unsubstituted position of the quinone electrophile OTQ that is produced from photoexcitation of OTA or OTHQ.<sup>38</sup> The OTHQ-GSH conjugate has been fully characterized previously using NMR spectroscopy and possesses a phenolic absorption at  $\lambda_{\max} = 352$  nm, and analysis by ESI-MS shows  $[M - H]^- = 689$  with a prominent fragment ion at  $m/z$  416 from  $\beta$ -elimination of benzoquinol-SH;<sup>38</sup> an established fragmentation of S-peptide-benzoquinone adducts.<sup>39</sup> In this study, its identity was confirmed by UV-vis and ESI-MS analysis (Supporting Information).

The major conjugate produced from the photoreaction of OTA with GSH is OTB-GSH. This species has a phenolic absorption at  $\lambda_{\max} = 331$  nm and a parent ion at  $[M - H]^- = 673$ ; 16 mass units less than OTHQ-GSH. The conjugate also undergoes  $\beta$ -elimination of benzoquinol-SH to afford a fragment ion at  $m/z$  400, which is 32 mass units heavier than OTB ( $[M - H]^- = 368$ ). These UV-vis and ESI-MS characteristics are consistent with the OTB-GSH structure shown in Figure 1 with replacement of the C5-Cl atom by the S atom of GSH. The corresponding cysteine (CySH) conjugate of OTA (OTB-CySH) has been previously characterized, and it also shows a prominent fragment ion at  $m/z$  400 and a phenolic absorption at  $\lambda_{\max} = 330$  nm.<sup>33</sup>

The photoreaction of OTBr with GSH (Figure 3B) showed the same products as the OTA reaction, despite OTBr being more photoreactive than OTA and undergoing complete photodegradation during the 15 min of irradiation time of the experiment. OTBr was used as a mixture of diastereomers [3(R/S), Figure 1], and so, two separable peaks were observed for the photoproducts OTB and OTHQ (Figure 3B). However, upon attachment of GSH to generate OTB-GSH and OTHQ-GSH, the stereoisomers were not separable by HPLC using the conditions for Figure 3. In contrast to OTA and OTBr, OTB failed to react with GSH upon photoirradiation (Figure 3C), while OTHQ produced OTHQ-GSH (Figure 3D) from reaction of GSH with the quinone electrophile OTQ that is generated from irradiation of OTHQ.<sup>38</sup>

These differences in photoreactivity for the ochratoxins were also evident from their reactions with dG.<sup>40</sup> Both OTA and OTBr react with dG to generate the C-linked OTB-dG adduct (Figure 1) that has been previously characterized by NMR spectroscopy<sup>29</sup> and recently shown to be present in samples of rat kidney DNA.<sup>27</sup> OTB failed to react with dG upon irradiation, while OTHQ produced a trace amount of an adduct designated as OTHQ-dG that does not comigrate with OTB-dG and exhibits a very different UV spectrum with  $\lambda_{\max} = 376$  nm.<sup>40</sup> On the basis of the mass of the adduct that had a parent ion at  $[M - H]^- = 631$ , which is two mass units less than OTB-dG, OTHQ-dG was ascribed to a benzetheno type adduct from reaction of dG with the quinone electrophile OTQ.<sup>40</sup> Representative HPLC traces from the photoreaction (15 min) of the ochratoxins (1 mM) with excess (40 equiv) dG is shown in Supporting Information (Figure S1). In Table 1 are given retention times (RT),  $\lambda_{\max}$  values,  $[M - H]^-$  ions, and fragment ions for the ochratoxins, GSH conjugates, and dG adducts.

**DNA Adduction.** Further insight into the role of the C5-X substituent in OTA reactivity was derived from study of DNA adduction by OTB and OTBr in human bronchial epithelial



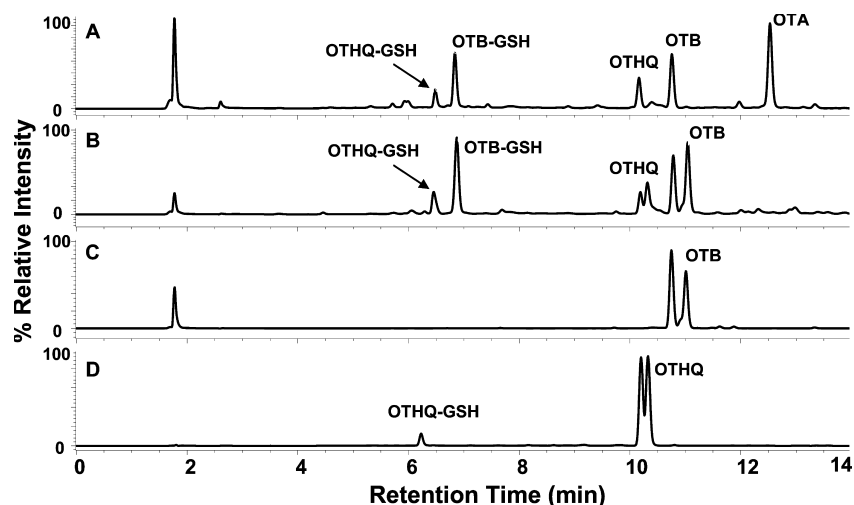


**Figure 3.** HPLC chromatograms [70:30 (0.1% formic acid in H<sub>2</sub>O–0.1% formic acid in ACN) to 25:75 in 17 min by a linear gradient] following 15 min of irradiation (350 nm) of 1 mM (A) OTA, (B) OTBr, (C) OTB, and (D) OTHQ in 50 mM phosphate buffer, pH 7.4, containing 15 equiv of GSH. OTHQ-GSH has been previously characterized,<sup>38</sup> while OTB-GSH is analogous to the previously characterized OTB-CySH conjugate.<sup>33</sup>

**Table 1. Spectral Data for Photoreactions of Ochratoxins with GSH and dG<sup>a</sup>**

species	RT (min) <sup>b</sup>	$\lambda_{\max}$ <sup>c</sup>	[M – H] <sup>–</sup>	fragment ions (m/z)
OTA	13.3	333	402	358, 314
OTBr	13.6, 14.1	332	446	402, 358
OTB	11.6, 11.9	320	368	324, 280
OTHQ	10.9, 11.0	350	384	340, 296
OTB-GSH	6.8	331	673	672, 544, 400
OTHQ-GSH	6.2	352	689	688, 560, 416
OTB-dG	7.5	326	633	517, 473, 429
OTHQ-dG	6.9, 7.0	376	631	515

<sup>a</sup>Photoreactions of ochratoxins (1 mM) in the presence of 15 molar equiv of GSH or 40 molar equiv of dG were carried out in 50 mM phosphate buffer, pH 7.4, for 15 min with irradiation at 350 nm using a Rayonet Chamber Reactor, model RPR-200. <sup>b</sup>Retention time, HPLC performed using an Agilent C-18 5  $\mu$  150 mm  $\times$  4.6 mm column with a flow rate of 0.75 mL/min using the following mobile phase: 70:30 (0.1% formic acid in H<sub>2</sub>O–0.1% formic acid in ACN) to 25:75 in 17 min by a linear gradient. <sup>c</sup>Phenolic ring absorbance in nm.

(WI26) and human kidney (HK2) cell lines. These cell lines were used previously to study DNA adduct formation by OTA and OTHQ.<sup>30</sup> For both OTA and OTHQ, low levels of DNA adducts (8–10 adducts/10<sup>9</sup> nucleotides) were detected by <sup>32</sup>P-postlabeling following treatment of WI26 and HK2 cells with 1  $\mu$ M toxin for various lengths of time (2, 7, and 24 h).<sup>30</sup> Figure 4 shows the adduct pattern obtained following OTB (1  $\mu$ M) or OTBr (1  $\mu$ M) treatment of WI26 cells, while the corresponding adduct pattern in HK2 cells is shown in Figure 5. For the nonchlorinated OTB (C5–X = H, Figure 1) analogue, no adduct spots were detected in WI26 (Figure 4) or HK2 (Figure 5) cells. In contrast, OTBr was found to form DNA adducts in WI26 (Figure 4) and HK2 (Figure 5) cells. Faint adduct spots were detected, especially after 6 h of incubation, as indicated by the arrows in Figures 4 and 5.

**Cytotoxicity.** The MTT assay was performed to determine the cytotoxicity of the ochratoxins (OTA, OTBr, OTB, and OTHQ) in OK, WI26, and HK2 cells. For these assays, the cells were treated with increasing amounts of ochratoxin (0.05–25  $\mu$ M), and the survival rate was measured after 48 h of

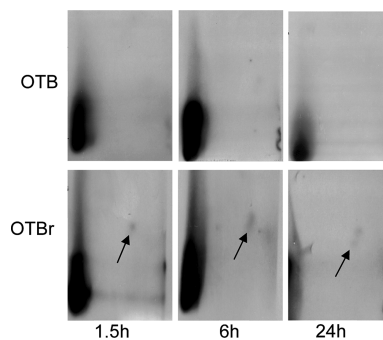


**Figure 4.** TLC maps of <sup>32</sup>P-labeled DNA adducts obtained following treatment of WI26 with 1  $\mu$ M OTB or OTBr for 1.5, 6, and 24 h.

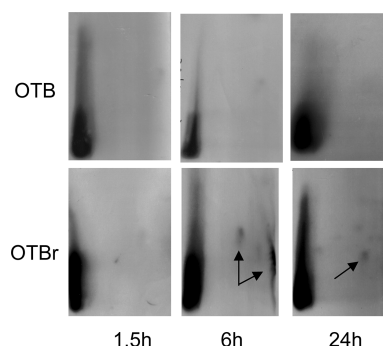


**Figure 5.** TLC maps of <sup>32</sup>P-labeled DNA adducts obtained following treatment of HK2 with 1  $\mu$ M OTB or OTBr for 1.5, 6, and 24 h.

exposure (Figure 6). The data presented in Figure 6 show the natural OTA to be the most cytotoxic of all analogues, showing cytotoxicity in all cell lines in the high-dose exposure regime (10, 25  $\mu$ M). OK cells were the most susceptible to OTA-mediated cytotoxicity (Figure 6A) followed by WI26 (Figure 6B) and then HK2 (Figure 6C) cells that only showed cytotoxicity at 10 and 25  $\mu$ M OTA exposure. As reported previously, OTB is also cytotoxic to OK cells but not to the same degree as OTA (Figure 6A).<sup>36</sup> In this cell line, OTBr

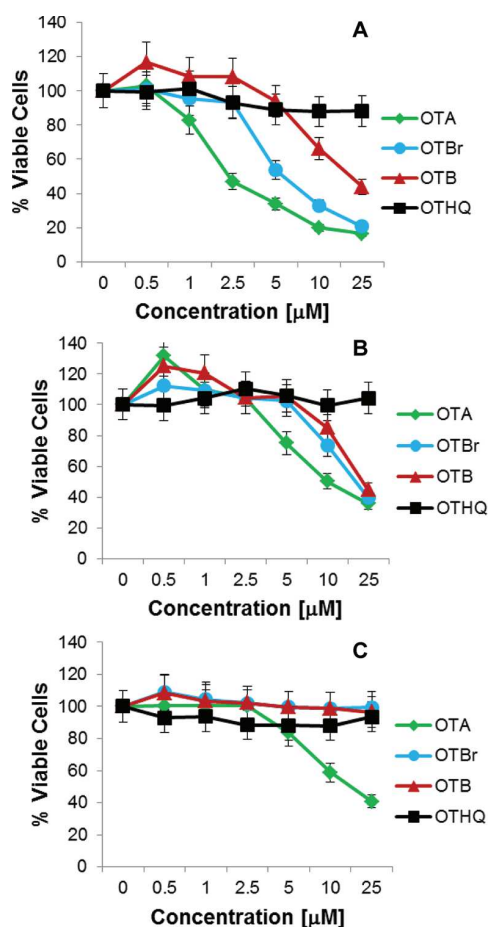


**Figure 6.** Viability of (A) OK, (B) W126, and (C) HK2 cells after 48 h of exposure with 0.5, 1, 2.5, 5, 10, and 25  $\mu\text{M}$  OTA, OTBr, OTB, and OTHQ obtained using the MTT assay. Mean values (SD) were obtained in six independent experiments.

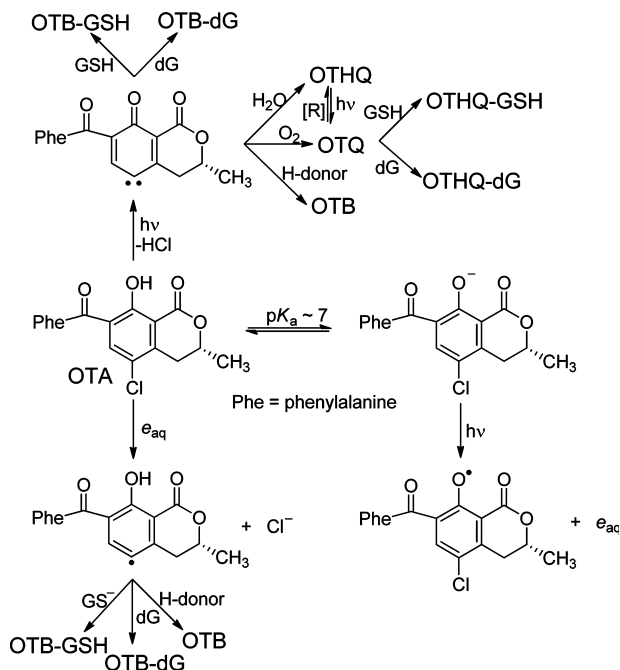
shows similar cytotoxicity to OTA at high doses, while the hydroquinone OTHQ failed to show cytotoxicity. In W126 cells, high doses (25  $\mu\text{M}$ ) of OTB and OTBr were as cytotoxic as OTA (Figure 6B), while again OTHQ failed to show cytotoxicity. In HK2 cells (Figure 6C), only OTA showed measurable cytotoxicity.

## DISCUSSION

To determine SAR for the ochratoxins shown in Figure 1, we first assessed their photoreactivity in the absence (Figure 2) and presence of GSH (Figure 3) or dG (Figure S1). Our choice of GSH and dG as representative biological nucleophiles stemmed from our previous studies showing that the parent OTA reacts covalently with GSH to generate OTHQ-GSH.<sup>38</sup> Experiments carried out by Obrecht-Pflumio and Dirheimer also suggested that OTA forms guanine-specific DNA adducts,<sup>41,42</sup> and we have shown that OTA reacts photochemically with dG to form OTB-dG.<sup>29</sup> Thus, the impact of the C5 substituent on reactivity toward GSH and dG could be determined. Our previous studies have also shown that the product distribution from OTA photochemistry is analogous to the photoproducts of 4-chlorophenol (4-ClPhOH).<sup>34,37</sup> Heterolysis of the C-Cl bond to form a carbene intermediate is well documented for the protonated form of 4-ClPhOH.<sup>43,44</sup> However, the phenolate of

4-ClPhOH undergoes photoionization to yield solvated electrons ( $e_{\text{aq}}$ ) and the phenolic radical.<sup>44</sup> For OTA with a phenolic  $\text{pK}_a \sim 7$ ,<sup>45</sup> the transient absorption spectrum immediately after photoexcitation is dominated by the absorption spectrum of  $e_{\text{aq}}$  that reacts with OTA.<sup>34</sup> Thus, as outlined in Scheme 1, this has led to the speculation that the

### Scheme 1. Proposed Pathways of OTA Photoreactions



photochemistry of the OTA phenolate leads to reductive dehalogenation of the toxin with homolytic cleavage of the C-Cl bond to generate  $\text{Cl}^-$  and an aryl radical in addition to the phenoxyl radical that is formed in the initial photoionization process.<sup>34</sup> The protonated form of OTA is still expected to undergo C-Cl bond heterolysis to generate a carbene intermediate,<sup>34</sup> as noted for 4-ClPhOH.<sup>43,44</sup>

The SARs for the photodecomposition of the ochratoxins presented in Figure 2 are consistent with the hypothesis that cleavage of the C5-X bond initiates the photodecomposition process.<sup>34</sup> The energy required for homolytic bond cleavage for aromatic compounds ( $\text{C}_6\text{H}_5\text{-X}$ ) bearing different X substituents has been tabulated by Blanksby and Ellison in  $\text{kcal mol}^{-1}$ :  $\text{C}_6\text{H}_5\text{-H}$  ( $112.9 \pm 0.5$ ),  $\text{C}_6\text{H}_5\text{-OH}$  ( $112.4 \pm 0.6$ ),  $\text{C}_6\text{H}_5\text{-Cl}$  ( $97.1 \pm 0.6$ ), and  $\text{C}_6\text{H}_5\text{-Br}$  ( $84 \pm 1$ ).<sup>46</sup> Clearly, the C-Br bond is the weakest, followed by C-Cl and then C-OH and C-H, which are of equal stability. Both OTB and OTHQ were resistant to photodecomposition (Figure 2) because they lack a suitable leaving group to undergo C5-X bond cleavage either through heterolysis or homolytic cleavage. In contrast, OTBr is more photoreactive than OTA because the C5-Br bond is more labile than the corresponding C5-Cl bond in OTA.

Cleavage of the C5-X bond in OTA also provides a rationale for the products generated in the presence of GSH (Figure 3) or dG (Figure S1). For OTA, irradiation of the protonated species is expected to generate the carbene intermediate. Reaction of the carbene with an H-donor generates OTB, while reaction with  $\text{O}_2$  generates the benzoquinone OTQ and reaction with  $\text{H}_2\text{O}$  generates the hydroquinone OTHQ (Scheme 1).<sup>34,37</sup>

The stable OTB and OTHQ products were detected (Figures 3 and S1), while OTQ is too reactive for detection in aqueous media at physiological pH.<sup>32</sup> The quinone electrophile OTQ is also generated from photoirradiation of OTHQ,<sup>38</sup> and it reacts covalently with GSH to generate OTHQ-GSH (Figure 3)<sup>38</sup> and with dG to form OTHQ-dG (Figure S1 and Table 1).<sup>40</sup> Direct reaction of the OTA-carbene with GSH would give rise to OTB-GSH, while reaction with dG would furnish OTB-dG. These species may also be generated from the aryl radical intermediate formed by reduction of OTA by  $e_{aq}^-$ .<sup>34</sup> Aryl radicals are known to react covalently with dG to generate C8-dG adducts,<sup>47</sup> while nucleophilic attachment of  $GS^-$  by an  $S_{RN}1$  process<sup>48</sup> would yield OTB-GSH.

Given that product formation from photoirradiation of OTA stems from cleavage of the C5-Cl bond (Scheme 1), it is not surprising that the same products were generated from the more reactive bromo-analogue OTBr (Figures 3 and S1). However, the nonhalogenated analogue OTB failed to react with GSH and dG following photoirradiation. For simple phenols, photoionization to generate phenoxyl radicals and  $e_{aq}^-$  is the primary photoprocess, especially when the phenols are deprotonated.<sup>43</sup> The C5 substituent of the ochratoxins influences the phenolic  $pK_a$ , and a  $pK_a$  value  $\sim 8$  has been estimated for OTB.<sup>45</sup> Thus, at pH 7.4 (conditions of the photoreactions), sufficient OTB phenolate is present that the photoreaction is expected to generate the OTB phenoxyl radical and  $e_{aq}^-$ . Because OTB lacks a leaving group, it cannot interact with  $e_{aq}^-$  to generate an aryl radical, nor will it undergo C5-H heterolysis to yield a carbene intermediate. This leaves the OTB phenoxyl radical as the reactive species, and it is expected to be quenched by GSH through an H-atom abstraction process to regenerate OTB and produce the thiyl radical of GSH ( $GS^\bullet$ ).<sup>15</sup> The OTB phenoxyl radical is also unreactive toward covalent attachment to dG, given the lack of product formation from the photoreaction (Figure S1C). For the hydroquinone derivative OTHQ, which also has a phenolic  $pK_a \sim 8$ ,<sup>32</sup> the photoreaction will generate a semiquinone radical that can undergo a further oxidative process to generate the quinone electrophile OTQ.<sup>32</sup> The quinone electrophile OTQ reacts covalently with GSH to generate OTHQ-GSH (Figure 3)<sup>38</sup> and with dG (Figure S1D)<sup>40</sup> and DNA in cell cultures.<sup>30</sup>

The photochemistry of the ochratoxins highlights the impact of the C5 substituent. Photoirradiation of OTA generates electrophiles capable of reacting covalently with GSH (Figure 3)<sup>38</sup> and dG (Figure S1).<sup>29</sup> Not surprisingly, the C5-Cl atom of OTA can be replaced with a Br atom (OTBr) without change in chemical reactivity. However, replacement of the C5-Cl with an OH group (OTHQ) alters the photochemistry to one now dominated by the quinone electrophile OTQ where the photoproducts stem from Michael addition instead of attachment to the C5 position. Complete removal of the C5-Cl atom to yield OTB removes the production of electrophiles capable of reacting covalently with GSH (Figure 3C) or dG (Figure S1C).

A correlation between the photochemistry of the ochratoxins and their ability to form DNA adducts in cell cultures was observed. The analogues that can react with dG following photoirradiation (OTA, OTBr, and OTHQ, Figure S1) also react with DNA in cell cultures to generate covalent DNA adducts, as evidenced by <sup>32</sup>P-postlabeling. OTB fails to show DNA adduct formation under conditions where OTA,<sup>30</sup> OTBr (Figures 4 and 5), and OTHQ<sup>30</sup> generate adduct spots in both

WI26 and HK2 cells. These results suggest that OTB lacks direct genotoxicity, while OTA, OTBr, and OTHQ can be viewed as direct genotoxins, ochratoxins capable of forming covalent DNA adducts.

For induction of OTA cytotoxicity, recent studies have shown a close correlation between the onset of oxidative DNA damage.<sup>17,19,20</sup> These studies have employed the comet assay (single cell gel electrophoresis) to indirectly detect oxidative DNA damage mediated by OTA with the aid of the repair enzyme formamido-pyrimidine-DNA-glycosylase (Fpg). The enzyme Fpg cleaves DNA at a variety of oxidized guanine adducts, producing DNA fragmentation. The onset of OTA-induced cytotoxicity in cell cultures is highly correlated with the induction of enhanced DNA breakage by the comet assay following Fpg treatment.<sup>17,19,20</sup> This suggests that oxidative DNA damage mediated by ROS is responsible for the observed cytotoxicity, given that OTA has been shown to stimulate ROS production in bacteria, rat liver microsomes, mitochondria, and rat hepatocytes.<sup>49,50</sup> In HK2 cells, ROS generated by OTA treatment were determined by using the fluorescent probe dihydrodichlorofluorescein diacetate (H2DCF-DA).<sup>19</sup> Following 6 h of OTA exposure, an increased level of ROS was observed. Pretreatment of the cells with *N*-acetylcysteine (NAC) showed a significant decrease in ROS levels, resulting in a significant increase in cell viability at all concentrations of OTA tested.<sup>19</sup> These studies have firmly established that oxidative DNA damage causes OTA-mediated cytotoxicity.<sup>17,19,20</sup>

Previous studies carried out in cultured cells have also shown cells to display a range of sensitivities to OTA-mediated cytotoxicity.<sup>19,20</sup> In our experiments, the viability of OK cells was strongly decreased by OTA concentrations  $>2.5 \mu M$ , whereas WI26 and HK2 cells were more resistant (Figure 6). In OK cells, the decrease in cell number mediated by OTA is due to apoptosis and necrosis.<sup>51</sup> OK cells lack sulfotransferase enzymes.<sup>36</sup> In contrast, WI26 and HK2 cells are of human origin and contain all metabolic capacity. Thus, the heightened sensitivity of OK cells to OTA-mediated cytotoxicity may be due to the lack of OTA sulfoconjugation.

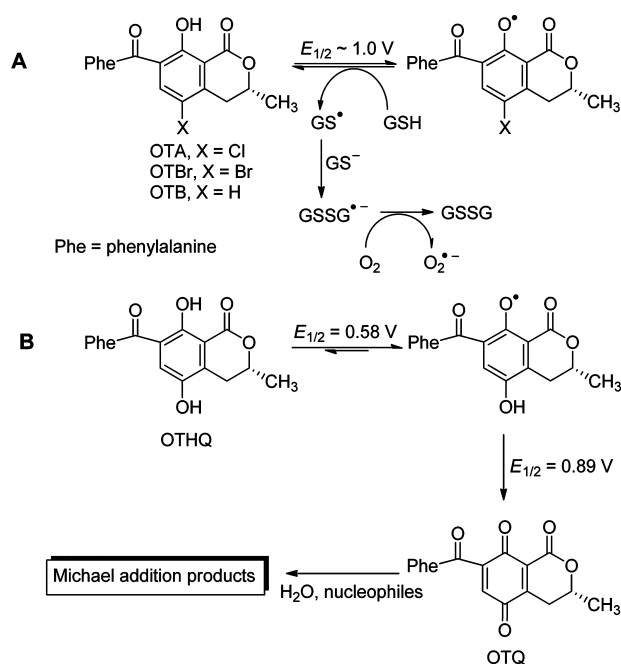
Interestingly, a correlation between photoreactivity and cytotoxicity was not observed. In OK and WI26 cells, OTBr and OTB displayed cytotoxicity at a level similar to OTA at  $25 \mu M$ , while the hydroquinone OTHQ failed to exhibit cytotoxicity (Figure 6). In HK2 cells, all of the synthetic samples (OTBr, OTB, and OTHQ) failed to exhibit cytotoxicity under the conditions employed. One factor that can play a role in cytotoxicity is stereochemistry, and the synthetic samples of OTBr, OTB, and OTHQ were used as mixtures of diastereomers [3(*R/S*), Figure 1], while the natural product OTA was a stereochemically pure sample. However, recent results show that the *L*-configuration of the phenylalanine moiety of OTA is important for cytotoxicity, while the stereocenter at the dihydroisocoumarin structure is of less importance,<sup>52</sup> suggesting that use of the diastereomer mixture for OTHQ did not play a dramatic role in its inability to induce cytotoxicity.

Oxidative DNA damage and hence cytotoxicity mediated by OTA are expected to result from direct redox cycling reactions involving OTA, coupled to indirect mechanisms resulting from reduction of cellular antioxidant defenses, which is expected to amplify the oxidative-mediated effects of OTA.<sup>21</sup> OTA contains a phenolic ring system, and a potential mechanism for oxidative stress mediated by phenols has been described as futile thiol

pumping.<sup>53,54</sup> This generates ROS, thiol oxidation, and antioxidant depletion, and OTA is known to reduce GSH levels in mammalian cell lines<sup>17</sup> and stimulate ROS production.<sup>19,49,50</sup> Such direct redox cycling pathways are initiated by production of the phenoxyl radical,<sup>53,54</sup> and electrochemical measurements show that OTA undergoes a 1e oxidative process in aqueous media to form the phenoxyl radical at  $E_{1/2} = 1.04$  V vs NHE.<sup>55</sup> Peroxidase enzymes are deemed important for OTA bioactivation,<sup>56,57</sup> and peroxidases are well-known to catalyze the conversion of phenols into phenoxyl radicals.<sup>58,59</sup>

The pathways in Scheme 2 permit a rationale for the role of the C5–X substituent in OTA-mediated cytotoxicity (Figure

**Scheme 2. Proposed Pathways for (A) ROS Generation by OTA, OTBr, and OTB and (B) Lack of ROS Generation by OTHQ**



6). Replacement of the C5–Cl atom with Br or H will not dramatically impact the reactivity of the phenoxyl radical, given that the phenolates of PhOH, 4-ClPhOH, and 4-BrPhOH have almost identical 1e oxidative potentials ( $E^{\circ} \sim 0.85$  V vs NHE).<sup>60</sup> Thus, for OTA, OTBr, and OTB the redox cycling pathway in Scheme 2A should take place, and these ochratoxins should be cytotoxic, as observed in OK and WI26 cells (Figure 6A,B). In contrast, replacement of the C5–Cl atom with OH to generate OTHQ does have a dramatic impact on the reactivity of the phenoxyl radical. OTHQ undergoes a 1e oxidative process in aqueous media to form the phenoxyl radical (semiquinone radical) at  $E_{1/2} = 0.58$  V vs NHE.<sup>55</sup> Thus, the semiquinone radical of OTHQ is a much weaker oxidant than the phenoxyl radicals of OTA, OTBr, and OTB and is less likely to be reduced by GSH (Scheme 2B). Instead, a second 1e oxidative process occurs at  $E_{1/2} = 0.89$  V vs NHE that is ascribed to oxidation of the semiquinone radical into the quinone electrophile OTQ (Scheme 2B).<sup>55</sup>

In general, hydroquinone/quinone redox couples are well-known to stimulate cytotoxicity,<sup>61–63</sup> although it is difficult to separate the biological effects caused by Michael adduct

formation from that of ROS generation.<sup>64</sup> An accepted mechanism for quinone-mediated oxidative stress involves reduction of the quinone by reductases to a semiquinone radical, which reduces oxygen to O<sub>2</sub><sup>•-</sup> and reforms the quinone.<sup>61–63</sup> This futile redox cycling forms cytotoxic levels of H<sub>2</sub>O<sub>2</sub>, and GSSG is retained by the cell and causes cytotoxic mixed protein disulfide formation.<sup>63</sup> Our studies on the OTHQ/OTQ redox couple show OTQ to be an arylating quinone with the C6 position available for Michael adduct formation.<sup>38</sup> We have also found OTQ to be highly reactive, undergoing decomposition in aqueous media to form a polar diacid derivative.<sup>32</sup> Thus, as outlined in Scheme 2B, it is expected that once OTQ is formed it will react immediately with H<sub>2</sub>O and biological nucleophiles, making its formation from the semiquinone radical essentially irreversible. This concept has been demonstrated for other arylating quinones; that is, quinones with higher chemical reactivity display lower cytotoxicity due to more rapid detoxification by Michael addition reactions.<sup>64</sup> This concept provides a rationale for lack of cytotoxicity displayed by OTHQ (Figure 6).

The C5–X substituent of OTA also plays a role in OTA metabolism.<sup>65,66</sup> OTA is cleaved by carboxypeptidase A to the nontoxic ochratoxin  $\alpha$  (OT $\alpha$ ) and phenylalanine (Phe), leading to detoxification.<sup>65,66</sup> OTB is cleaved much quicker by this enzyme,<sup>65,66</sup> while OTBr undergoes hydrolysis at a rate comparable to OTA.<sup>66</sup> That OTB undergoes hydrolysis by carboxypeptidase at a quicker rate than OTA has been evoked as a rationale for its lower toxicity.<sup>67</sup> In these studies, administration of OTB to male rats failed to induce major histopathological features in the kidneys (karyomegaly and apoptosis of tubular epithelial cells in the outer stripe of the outer medulla) that is characteristic of OTA-mediated nephrotoxicity.<sup>6,28</sup> Because differences in toxicokinetics between OTA and OTB were viewed to be responsible for their different potential to induce nephrotoxicity, the cytotoxicities of OTA and OTB were compared in a cell system where toxicokinetics play a minor role.<sup>67</sup> The cytotoxicity of OTA was more pronounced only at low concentrations; at higher concentrations, both OTA and OTB induced a similar reduction in cell viability (i.e., Figure 6B), suggesting that these two analogues are equally cytotoxic.<sup>67</sup> Additional experiments carried out in rats also showed that OTB generates a similar degree of DNA breakage at the same dose of OTA,<sup>68</sup> and that the C5–Cl atom of OTA is not a structural requirement for OTA-mediated cytotoxicity.<sup>67,68</sup>

Our findings show that the C5–Cl atom is critical for direct genotoxicity mediated by OTA but plays a lesser role in OTA-mediated cytotoxicity. Thus, cytotoxicity is not a true measure of OTA reactivity and overall toxicity to cells. The new findings on OTA mutagenicity favor direct genotoxicity and rule out oxidative DNA damage as a contributor to induction of deletion mutations or renal carcinogenesis.<sup>28</sup> However, oxidative DNA damage is regarded as the contributor to the induction of OTA-mediated cytotoxicity.<sup>17,19,20</sup> Our SAR for OTA photoreactivity, DNA adduction, and cytotoxicity in mammalian cells is consistent with different MOAs for OTA-mediated cytotoxicity and direct genotoxicity. These data support the hypothesis that toxicity and carcinogenicity induced by OTA are driven by two different MOAs.<sup>69</sup>



## ASSOCIATED CONTENT

ESI-MS spectra of GSH and dG adducts derived from photoirradiation of the ochratoxins and Figure S1 described in the text. This material is available free of charge via the Internet at <http://pubs.acs.org>.

## AUTHOR INFORMATION

### Corresponding Author

\*E-mail: [leszkowicz@ensat.fr](mailto:leszkowicz@ensat.fr) (A.P.-L.) or [rmanderv@uoguelph.ca](mailto:rmanderv@uoguelph.ca) (R.A.M.).

### Author Contributions

<sup>§</sup>These authors contributed equally to this work.

### Funding

Support for this research was provided by the European Union ("Ochratoxin A-risk assessment" QLK1-2001-01614), the Region Midi-Pyrénées, the French Ministry of Research, the Association recherche cancer (ARC), Natural Sciences and Engineering Research Council of Canada (NSERC), the Canadian Foundation for Innovation (CFI), and the Ontario Innovation Trust Fund (OIT).

## ACKNOWLEDGMENTS

We thank Dr. Wojciech Gabryelski (University of Guelph) for assistance with the mass spectral analysis.

## ABBREVIATIONS

OTA, *N*-[[(3*R*)-5-chloro-8-hydroxy-3-methyl-1-oxo-3,4-dihydro-1*H*-isochromen-7-yl]carbonyl]-*L*-phenylalanine; OTBr, *N*-{[(3*R,S*)-5-bromo-8-hydroxy-3-methyl-1-oxo-3,4-dihydro-1*H*-isochromen-7-yl]carbonyl}-*L*-phenylalanine; OTB, *N*-{[(3*R,S*)-8-hydroxy-3-methyl-1-oxo-3,4-dihydro-1*H*-isochromen-7-yl]carbonyl}-*L*-phenylalanine; OTHQ, *N*-{[(3*R,S*)-5,8-dihydroxy-3-methyl-1-oxo-3,4-dihydro-1*H*-isochromen-7-yl]carbonyl}-*L*-phenylalanine; SAR, structure-activity relationships; MOA, mechanism of action; dG, 2'-deoxyguanosine; 4-ClPhOH, 4-chlorophenol; OK, opossum kidney epithelial cells; WI26, human bronchial epithelial cells; HK2, human kidney cells; D-EMEM, Dulbecco's Eagle's minimum essential medium; RPMI, Roswell Park Memorial Institute medium.

## REFERENCES

- (1) van der Merwe, K. J., Steyn, P. S., Fourie, L., Scott, D. B., and Theron, J. J. (1965) Ochratoxin A, a toxic metabolite produced by *Aspergillus ochraceus* Wilh. *Nature* 205, 1112–1113.
- (2) Pohland, A. E., Nesheim, S., and Friedman, L. (1992) Ochratoxin A, a review. *Pure Appl. Chem.* 64, 1029–1046.
- (3) Pfohl-Leszkowicz, A., and Manderville, R. A. (2007) Ochratoxin A: An overview on toxicity and carcinogenicity in animals and humans. *Mol. Nutr. Food Res.* 51, 61–99.
- (4) Mally, A., and Dekant, W. (2009) Mycotoxins and the kidney: Modes of action for renal tumor formation by ochratoxin A in rodents. *Mol. Nutr. Food Res.* 53, 467–478.
- (5) Kuiper-Goodman, T., Hiltz, C., Billiard, S. M., Kiparissis, Y., Richard, I. D. K., and Hayward, S. (2010) Health risk assessment of ochratoxin A for all age-sex strata in a market economy. *Food Addit. Contam.* 27, 212–240.
- (6) Boorman, G., Ed. (1989) NTP Technical Report on the Toxicology and Carcinogenesis Studies of Ochratoxin A (CAS No. 303-47-9) in F344/N Rats (Gavage Studies). *NIH Publication No. 89-2813*, U.S. Department of Health and Human Services, National Institutes of Health, Research Triangle Park, NC.
- (7) Stoev, S. D. (2010) Studies on carcinogenic and toxic effects of ochratoxin A in chicks. *Toxins* 2, 649–664.

- (8) IARC (1993) *Monographs on the Evaluation of Carcinogenic Risks to Humans. Some Naturally Occurring Substances: Food Items and Constituents, Heterocyclic Aromatic Amines and Mycotoxins*, No. 56, Ochratoxin A, pp 489–521, International Agency for Research on Cancer, Lyon.

- (9) Bolt, H. M., Foth, H., Hengstler, J. G., and Degen, G. H. (2004) Carcinogenicity categorization of chemicals-new aspects to be considered in a European perspective. *Toxicol. Lett.* 151, 29–41.

- (10) Bolt, H. M., and Degen, G. H. (2004) Human carcinogenic risk evaluation, part II: Contributions of the EUROTOX specialty section for carcinogenesis. *Toxicol. Sci.* 81, 3–6.

- (11) JECFA (2001) *Safety Evaluation of Certain Mycotoxins in Food, Fifty-Sixth Meeting of the Joint FAO/WHO Expert Committee on Food Additives (JECFA)*, WHO Food Additives Series, Vol. 47, pp 281–415, World Health Organization, Geneva.

- (12) Kuiper-Goodman, T. (1996) Risk assessment of ochratoxin A: an update. *Food Addit. Contam.* 13 (Suppl.), 53–57.

- (13) Lock, E. A., and Hard, G. C. (2004) Chemically induced renal tubule tumors in the laboratory rat and mouse: Review of the NCI/NTP database and categorization of renal carcinogens based on mechanistic information. *Crit. Rev. Toxicol.* 34, 211–299.

- (14) Turesky, R. J. (2005) Perspective: Ochratoxin A is not a genotoxic carcinogen. *Chem. Res. Toxicol.* 18, 1082–1090.

- (15) Manderville, R. A. (2005) A case for the genotoxicity of ochratoxin A by bioactivation and covalent DNA adduction. *Chem. Res. Toxicol.* 18, 1091–1097.

- (16) Gautier, J.-C., Holzhaeuser, D., Markovic, J., Gremaud, E., Schilter, B., and Turesky, R. J. (2001) Oxidative damage and stress response from ochratoxin A exposure in rats. *Free Radical Biol. Med.* 30, 1089–1098.

- (17) Kamp, H. G., Eisenbrand, G., Schlatter, J., Würth, K., and Janzowski, C. (2005) Ochratoxin A: Induction of (oxidative) DNA damage, cytotoxicity and apoptosis in mammalian cell lines and primary cells. *Toxicology* 206, 413–425.

- (18) Kamp, H. G., Eisenbrand, G., Janzowski, C., Kiossev, J., Latendresse, J. R., Schlatter, J., and Turesky, R. J. (2005) Ochratoxin A induces oxidative DNA damage in liver and kidney after oral dosing to rats. *Mol. Nutr. Food Res.* 49, 1160–1167.

- (19) Arbillaga, L., Azqueta, A., Ezpeleta, O., and Lopez de Cerain, A. (2007) Oxidative DNA damage induced by Ochratoxin A in the HK-2 human kidney cell line: evidence of the relationship with cytotoxicity. *Mutagenesis* 22, 35–42.

- (20) Alia, R., Mittelstaedt, R. A., Shaddock, J. G., Ding, W., Bhalli, J. A., Khana, Q. M., and Heflich, R. H. (2011) Comparative analysis of micronuclei and DNA damage induced by ochratoxin A in two mammalian cell lines. *Mutat. Res.* 723, 58–64.

- (21) Marin-Kuan, M., Ehrlich, V., Delatour, T., Cavin, C., and Schilter, B. (2011) Evidence for a role of oxidative stress in the carcinogenicity of ochratoxin A. *J. Toxicol.* 2011, 1–15.

- (22) Pfohl-Leszkowicz, A., Chakor, K., Creppy, E. E., and Dirheimer, G. (1991) DNA-adduct formation in mice treated with ochratoxin A. In *Mycotoxins, Endemic Nephropathy and Urinary Tract Tumours* (Castegnaro, M., Plestina, R., Dirheimer, G., Chernozemsky, I. N., and Bartsch, H., Eds.) pp 245–253, IARC Scientific Publications No. 115, Lyon, France.

- (23) Pfohl-Leszkowicz, A., Grosse, Y., Kane, A., Creppy, E. E., and Dirheimer, G. (1993) Differential DNA adduct formation and disappearance in three mouse tissues after treatment with the mycotoxin ochratoxin A. *Mutat. Res.* 289, 265–273.

- (24) Grosse, Y., Baudrimont, I., Castegnaro, M., Creppy, E. E., Dirheimer, G., and Pfohl-Leszkowicz, A. (1995) Ochratoxin A metabolites and DNA-adducts formation in monkey kidney cell. *Chem.-Biol. Interact.* 95, 175–187.

- (25) Pfohl-Leszkowicz, A., Pinelli, E., Bartsch, H., Mohr, U., and Castegnaro, M. (1998) Sex and strain differences in ochratoxin A metabolism and DNA adduction in two strains of rats. *Mol. Carcinogen.* 23, 76–83.

- (26) Faucet, V., Pfohl-Leszkowicz, A., Dai, J., Castegnaro, M., and Manderville, R. A. (2004) Evidence for covalent DNA adduction by

ochratoxin A following chronic exposure to rat and subacute exposure to pig. *Chem. Res. Toxicol.* 17, 1289–1296.

(27) Mantle, P. G., Faucet-Marquis, V., Manderville, R. A., Squillaci, B., and Pfohl-Leszkowicz, A. (2010) Structures of covalent adducts between DNA and ochratoxin A: A new factor in debate about genotoxicity and human risk assessment. *Chem. Res. Toxicol.* 23, 89–98.

(28) Hibi, D., Suzuki, Y., Ishii, Y., Jin, M., Maiko Watanabe, M., Sugita-Konishi, Y., Yanai, T., Nohmi, T., Nishikawa, A., and Umemura, T. (2011) Site-specific *in vivo* mutagenicity in the kidney of *gpt* delta rats given a carcinogenic dose of ochratoxin A. *Toxicol. Sci.* 122, 406–414.

(29) Dai, J., Wright, M. W., and Manderville, R. A. (2003) Ochratoxin A forms a carbon-bonded C8-deoxyguanosine nucleoside adduct: Implications for C8 reactivity by a phenolic radical. *J. Am. Chem. Soc.* 125, 3716–3717.

(30) Tozlovanu, M., Faucet-Marquis, V., Pfohl-Leszkowicz, A., and Manderville, R. A. (2006) Genotoxicity of the hydroquinone metabolite of ochratoxin A: Structure-activity relationships for covalent DNA adduction. *Chem. Res. Toxicol.* 19, 1241–1247.

(31) Frenette, C., Paugh, R. J., Tozlovanu, M., Juzio, M., Pfohl-Leszkowicz, A., and Manderville, R. A. (2008) Structure-activity relationships for the fluorescence of ochratoxin A: Insight for detection of ochratoxin A metabolites. *Anal. Chim. Acta* 617, 153–161.

(32) Gillman, I. G., Clark, T. N., and Manderville, R. A. (1999) Oxidation of ochratoxin A by an Fe-porphyrin system: Model for enzymatic activation and DNA cleavage. *Chem. Res. Toxicol.* 12, 1066–1076.

(33) Brow, M. E., Dai, J., Park, G., Wright, M. W., Gillman, I. G., and Manderville, R. A. (2002) Photochemically catalyzed reaction of ochratoxin A with D- and L-cysteine. *Photochem. Photobiol.* 76, 649–656.

(34) Il'ichev, Y. V., Perry, J. L., Manderville, R. A., Chignell, C. F., and Simon, J. D. (2001) The pH-dependent primary photoreactions of ochratoxin A. *J. Phys. Chem. B* 105, 11369–11376.

(35) Reddy, M. V., and Randerath, K. (1986) Nuclease P1-mediated enhancement of sensitivity of <sup>32</sup>P-Postlabeling test for structurally diverse DNA adducts. *Carcinogenesis* 7, 1543–1551.

(36) Faucet-Marquis, V., Pont, F., Störmer, F., Rizk, T., Castegnaro, M., and Pfohl-Leszkowicz, A. (2006) Evidence of a new dechlorinated OTA derivative formed in opossum kidney cell cultures after pre-treatment by modulators of glutathione pathways. Correlation with DNA adducts formation. *Mol. Nutr. Food Res.* 50, 531–542.

(37) Gillman, I. G., Yezek, J. M., and Manderville, R. A. (1998) Ochratoxin A acts as a photoactivatable DNA cleaving agent. *Chem. Commun.*, 647–648.

(38) Dai, J., Park, G., Wright, M. W., Adams, M., Akman, S. A., and Manderville, R. A. (2002) Detection and characterization of a glutathione conjugate of ochratoxin A. *Chem. Res. Toxicol.* 15, 1581–1588.

(39) Mason, D. E., and Liebler, D. C. (2000) Characterization of benzoquinone-peptide adducts by electrospray mass spectrometry. *Chem. Res. Toxicol.* 13, 976–982.

(40) Manderville, R. A., and Pfohl-Leszkowicz, A. (2008) Bioactivation and DNA adduction as a rationale for ochratoxin A carcinogenesis. *World Mycotoxin J.* 1, 357–367.

(41) Obrecht-Pflumio, S., and Dirheimer, G. (2000) *In vitro* DNA and dGMP adducts formation caused by ochratoxin A. *Chem.-Biol. Interact.* 127, 29–44.

(42) Obrecht-Pflumio, S., and Dirheimer, G. (2001) Horseradish peroxidase mediates DNA and deoxyguanosine 3'-monophosphate adduct formation in the presence of ochratoxin A. *Arch. Toxicol.* 75, 583–590.

(43) Boule, P., Richard, C., David-Oudjehani, K., and Grabner, G. (1997) Photochemical behaviour of halophenols in aqueous solution. *Proc. Indian Acad. Sci.* 109, S09–S19.

(44) Grabner, G., Richard, C., and Köhler, G. (1994) Formation and reactivity of 4-oxocyclohexa-2,5-dienylidene in the photolysis of 4-

chlorophenol in aqueous solution at ambient temperature. *J. Am. Chem. Soc.* 116, 11470–11480.

(45) Arduo, J. A., Gillman, I. G., and Manderville, R. A. (1998) On the role of copper and iron in DNA cleavage by ochratoxin A. Structure-activity relationships in metal binding and copper-mediated DNA cleavage. *Can. J. Chem.* 76, 907–918.

(46) Blanksby, S. J., and Ellison, G. B. (2003) Bond dissociation energies of organic molecules. *Acc. Chem. Res.* 36, 255–263.

(47) Manderville, R. A. (2009) Structural and biological impact of radical addition reactions with DNA nucleobases. In *Advances in Physical Organic Chemistry* (Richard, J. P., Ed.) pp 177–218, Elsevier, Amsterdam.

(48) Galli, C., and Bunnett, J. F. (1981) Nucleophile Competition in Aromatic S<sub>RN</sub>1 Reactions. Evaluation of nucleophilic reactivities and evidence of reaction mechanism. *J. Am. Chem. Soc.* 103, 7140–7147.

(49) Hoehler, D., Marquardt, R. R., McIntosh, A. R., and Xiao, H. (1996) Free radical generation as induced by ochratoxin A and its analogs in bacteria (*Bacillus brevis*). *J. Biol. Chem.* 271, 27388–27394.

(50) Hoehler, D., Marquardt, R. R., McIntosh, A. R., and Hatch, G. M. (1997) Induction of free radicals in hepatocytes, mitochondria and microsomes of rats by ochratoxin A and its analogs. *Biochim. Biophys. Acta* 1357, 225–233.

(51) Sauvant, C., Holzinger, H., and Gekle, M. (2005) Proximal tubular toxicity of ochratoxin A is amplified by simultaneous inhibition of the extracellular signal-regulated kinases 1/2. *J. Pharmacol. Exp. Ther.* 313, 234–241.

(52) Cramer, B., Harrer, H., Nakamura, K., Uemura, D., and Humpf, H.-U. (2010) Total synthesis and cytotoxicity evaluation of all ochratoxin A stereoisomers. *Bioorg. Med. Chem.* 18, 343–347.

(53) Murray, A. R., Kisin, E., Castranova, V., Komminen, C., Gunther, M. R., and Shvedova, A. A. (2007) Phenol-induced *in vivo* oxidative stress in skin: Evidence for enhanced free radical generation, thiol oxidation, and antioxidant depletion. *Chem. Res. Toxicol.* 20, 1769–1777.

(54) Stoyanovskiy, D. A., Goldman, R., Jonnalagadda, S. S., Day, B. W., Claycamp, H. G., and Kagan, V. E. (1996) Detection and characterization of the electron paramagnetic resonance-silent glutathionyl-S,S-dimethyl-1-pyrroline N-oxide adduct derived from redox cycling of phenoxyl radicals in model systems and HL-60 cells. *Arch. Biochem. Biophys.* 330, 3–11.

(55) Calcutt, M. W., Gillman, I. G., Nofhle, R. E., and Manderville, R. A. (2001) Electrochemical oxidation of ochratoxin A: correlation with 4-chlorophenol. *Chem. Res. Toxicol.* 14, 1266–1272.

(56) Pinelli, E., Adlouni, C. E., Pipy, B., Quartulli, F., and Pfohl-Leszkowicz, A. (1999) Roles of cyclooxygenase and lipoxygenases in ochratoxin A genotoxicity in human epithelial lung cells. *Environ. Toxicol. Pharmacol.* 7, 95–107.

(57) Obrecht-Pflumio, S., Chassat, T., Dirheimer, G., and Marzin, D. (1999) Genotoxicity of ochratoxin A by Salmonella mutagenicity test after bioactivation by mouse kidney microsomes. *Mutat. Res.* 446, 95–102.

(58) Huang, Q., Huang, Q., Pinto, R. A., Griebenow, K., Schweitzer-Stenner, R., and Weber, W. J. Jr. (2005) Inactivation of horseradish peroxidase by phenoxyl radical attack. *J. Am. Chem. Soc.* 127, 1431–1437.

(59) Dai, J., Sloat, A. L., Wright, M. W., and Manderville, R. A. (2005) Role of phenoxyl radicals in DNA adduction by chlorophenol xenobiotics following peroxidase activation. *Chem. Res. Toxicol.* 18, 771–779.

(60) Li, C., and Hoffman, M. Z. (1999) One-electron redox potentials of phenols in aqueous solution. *J. Phys. Chem. B* 103, 6653–6656.

(61) Monks, T. J., Hanzlik, R. P., Cohen, G. M., Ross, D., and Graham, D. G. (1992) Contemporary issues in toxicology: Quinone chemistry and toxicity. *Toxicol. Appl. Pharmacol.* 112, 2–16.

(62) Bolton, J. L., Trush, M. A., Penning, T. M., Dryhurst, G., and Monks, T. (2000) Role of quinones in toxicology. *Chem. Res. Toxicol.* 13, 135–160.

- (63) O'Brien, P. J. (1991) Molecular mechanisms of quinone cytotoxicity. *Chem.-Biol. Interact.* 80, 1–41.
- (64) Wang, X., Thomas, B., Sachdeva, R., Arterburn, L., Frye, L., Hatcher, P. G., Cornwell, D. G., and Ma, J. (2006) Mechanism of arylating quinone toxicity involving Michael adduct formation and induction of endoplasmic reticulum stress. *Proc. Natl. Acad. Sci. U.S.A.* 103, 3604–3609.
- (65) Doster, R. C., and Sinnhuber, R. O. (1972) Comparative rates of hydrolysis of ochratoxins A and B *in vitro*. *Food Cosmet. Toxicol.* 10, 389–394.
- (66) Stander, M. A., Steyn, P. S., van der Westhuizen, F. H., and Payne, B. E. (2001) A kinetic study into the hydrolysis of the ochratoxins and analogues by carboxypeptidase A. *Chem. Res. Toxicol.* 14, 302–304.
- (67) Mally, A., Keim-Heusler, H., Amberg, A., Kurz, M., Zepnik, H., Mantle, P., Völkel, W., Hard, G. C., and Dekant, W. (2005) Biotransformation and nephrotoxicity of ochratoxin B in rats. *Toxicol. Appl. Pharmacol.* 206, 43–53.
- (68) Mally, A., Pepe, G., Ravoori, S., Fiore, M., Gupta, R. C., Dekant, W., and Mosesso, P. (2005) Ochratoxin A causes DNA damage and cytogenetic effects but no DNA adducts in rats. *Chem. Res. Toxicol.* 18, 1253–1261.
- (69) Pfohl-Leszkowicz, A, Bartsch, H., Azémar, B., Mohr, U., Estève, J., and Castegnaro, M. (2002) MESNA protects rats against nephrotoxicity but not carcinogenicity induced by ochratoxin A, implicating two separate pathways. *Facta Univ., Ser. Med. Biol.* 9, 57–63.